Radiation from high-intensity ultrashort-laser-pulse and gas-jet magnetized plasma interaction

Davoud Dorranian,* Mikhail Starodubtsev, Hiromichi Kawakami, Hiroaki Ito, Noboru Yugami, and Yasushi Nishida
Energy and Environmental Science, Graduate School of Engineering, Utsunomiya University, 7-1-2 Yoto, Utsunomiya Tochigi 321-8585 Japan

(Received 10 February 2003; revised manuscript received 2 May 2003; published 19 August 2003)

Using a gas-jet flow, via the interaction between an ultrashort high-intensity laser pulse and plasma in the presence of a perpendicular external dc magnetic field, the short pulse radiation from a magnetized plasma wakefield has been observed. Different nozzles are used in order to generate different densities and gas profiles. The neutral density of the gas-jet flow measured with a Mach-Zehnder interferometer is found to be proportional to back pressure of the gas jet in the range of 1 to 8 atm. Strength of the applied dc magnetic field varies from 0 to 8 kG at the interaction region. The frequency of the emitted radiation with the pulse width of 200 ps (detection limit) is in the millimeter wave range. Polarization and spatial distributions of the experimental data are measured to be in good agreement with the theory based on the $\mathbf{V_p}\times\mathbf{B}$ radiation scheme, where $\mathbf{V_p}$ is the phase velocity of the electron plasma wave and $\mathbf{B}$ is the steady magnetic field intensity. Characteristics of the radiation are extensively studied as a function of plasma density and magnetic field strength. These experiments should contribute to the development of a new kind of millimeter wavelength radiation source that is tunable in frequency, pulse duration, and intensity.

DOI: 10.1103/PhysRevE.68.026409 PACS number(s): 52.25.Xz, 52.35.Hr, 52.38.Kd, 52.90.+z

I. INTRODUCTION

Plasma-based radiation sources are expanding rapidly. The multimode nature of the plasma has the capability to convert different initial energies to coherent radiation through processes such as Raman scattering, harmonic generation, or photon acceleration [1–3]. We are studying a new kind of high-power tunable radiation source, where the short electromagnetic pulse is generated by a magnetized plasma wake.

When making such radiation sources the coupling between the wake and the electromagnetic radiation at the plasma boundary is very important. To cause the transmission coefficient field of the radiation to increase by decreasing the attenuation effect due to ramping the plasma density at the boundary, the boundary should be as sharp as possible. One of the most advanced ways to achieve this requirement is by using the gas-jet flow. Controlling the initial neutral density by gas-jet back pressure as well as using different kinds of nozzles to make a suitable geometry of density interaction medium has presented some interesting advantages in our experiments. Previous works on gas-jet sources have focused on studying homogeneous condensation and making cluster beams [4], and after that gas jets are widely used in the field of laser-plasma interaction, in areas such as laser particle acceleration [5,6], inertial confinement fusion [7,8], x-ray lasers [9], and high harmonic generation [10]. Each field requires its special geometry of gas expansion and density configuration. In our case because the magnetized plasma is generated as a source of coherent electromagnetic radiation so the spatial distribution of gas density is an important characteristic specifically uniform gas density inside the flow and sharp boundaries at the interaction region. Because the laser beam passes transversely across the puffed gas area and the radiation from the interaction region should be viewed by the diagnostics, it is also important that the interaction region should be outside the nozzle with sufficient distance from the tip of the nozzle. The reported works in this area were conducted mostly in very high back pressure range [11,12] but due to our main purpose, which is detecting the radiation from magnetized wake, according to laser pulse width and plasma density relation, the neutral gas densities lower than 10^{17} cm^{-3} are interested for obtaining the maximum wake amplitude.

In this paper, the effects of different gas-jet nozzles on the density distribution characteristics in the low pressure regime of He and N_2 gases are reported and also the experiments of the emitted radiation in millimeter wave range from gas-jet plasma wakes excited by ultrashort intense laser pulse are presented.

Before coming to the experimental results it is convenient to explain briefly the theoretical background related to the present experiment. In this radiation scheme, a large amplitude plasma wake is generated by an intense laser pulse or a relativistic electron bunch in the presence of a modest perpendicular dc magnetic field. The initial motion of plasma electrons due to the laser ponderomotive force make them rotate around the magnetic field lines and generate the electromagnetic (em) part in the wake with a nonzero group velocity. The magnetized wake propagates through the plasma and couples to vacuum at the plasma-vacuum boundary. The theory of radiation from the wakes excited by laser pulse in the magnetized plasma has been introduced by Yoshii *et al.* [13] and the characteristics of this radiation have been observed by Yugami *et al.* [14].

By applying the external magnetic field in the direction perpendicular to the laser beam path so $\mathbf{k}\perp\mathbf{B}_0$ and also the wave electric field $\mathbf{E}\perp\mathbf{B}_0$, radiation occurs in the extraordinary mode and the dispersion relation is given by $c^2k^2/\omega^2 = 1-(\omega_p^2/\omega^2)[(\omega^2-\omega_p^2)/(\omega^2-\omega_H^2)]$, which is plotted in Fig. 1 [15]. Radiation frequency is introduced by the inter-

*Email address: doran@plasma.ees.utsunomiya-u.ac.jp

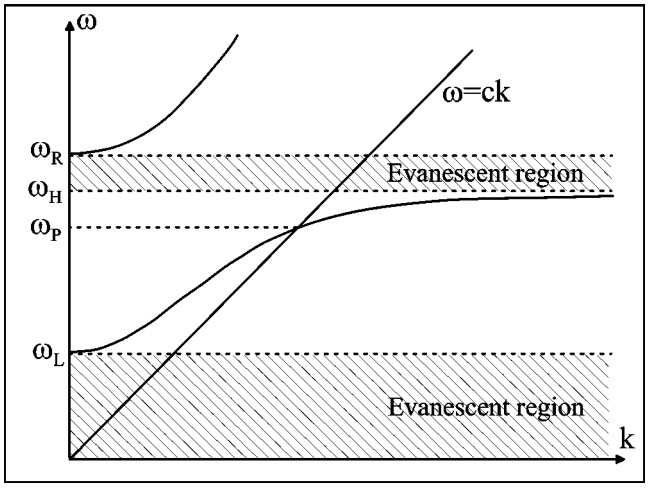

FIG. 1. Dispersion relation of the magnetized plasma. Evanescent regions are shown by dashed area.

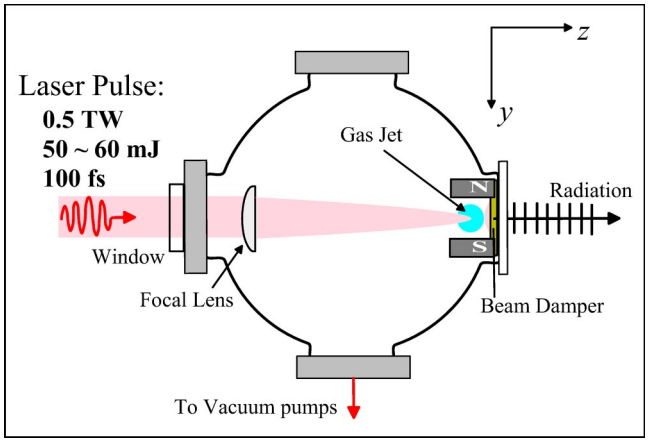

FIG. 2. Experimental setup.

section point between dispersion relation and laser pulse curves on ω-k diagram, where $\omega_P \leqq \omega < \omega_H$. Another parameter to guide the radiation through the plasma into vacuum is the boundary condition. In the case of gradual change of the plasma boundary, ω_H will gradually reduce toward the vacuum and the upper evanescent region in ω-k diagram will go down wider and wider. As a result, this area will cover all the radiation frequency range and the radiation should tunnel through this layer as it propagates into the vacuum, which makes the radiation power damp noticeably. In the case of sharp boundary plasma, on the other hand, according to the continuity of the tangential components of **E** of the reflected and the transmitted waves at the boundary, the transmission coefficient for E_x tends to 1. Using gas-jet plasma configuration with a suitable nozzle is a way to make the sharp plasma boundary. More details about the radiation theory can be found in Refs. [13,14,16] and the review will be given in the Appendix.

Section II describes the experimental setup. Section III is devoted to interferometry experiment and results. Radiation experiment results and discussions are presented in Sec. IV including theoretical background and finally a brief conclusion is presented in Sec. V.

II. EXPERIMENTAL SETUP

The experimental arrangement is shown schematically in Fig. 2. A mode locked Ti:sapphire laser operating at $\lambda_L = 800$ nm wavelength, with the pulse width of $\tau_L = 100$ fs [full width at half maximum (FWHM)], and maximum energy of 100 mJ per pulse with 10 Hz repetition rate is used to excite wakefield. The laser pulse is irradiated into the vacuum chamber through 5-mm-thickness CaF_2 window and is focused by a lens of $f/5$ at about 0.5 mm above the gas-jet nozzle. The focal spot diameter is about 20 μm and the intensity is of the order of 10^{17} W/cm^2. A solenoid valve (Iota one) made by Parker instrumentation with 0.8 mm diameter exit hole was employed to generate the gas-jet constant flow of 100~200 μs. These kind of valves are generally closed and the open time can be adjusted from 5 μs to several hours, in frequency or single-pulse mode. Gas jet synchronously operates with the laser pulse. Different nozzles are used in the experiment in order to change the gas density and also boundary configurations (Fig. 3). The strength of the applied magnetic field is up to 8 kG. As the region of the field along the $+z$ direction is about 2.5 cm, much longer than x_R, the Rayleigh length, it is expected to be uniform in the interaction region. The experiment is carried out using nitrogen and helium gases at the initial base pressure of below 5 mTorr and maximum gas-jet back pressure of 8 atm. The measurement system for the radiation consists of a crystal detector, horn antenna, waveguide, and oscilloscope (Tektronix; TDS-694C) with limitation of minimum pulse width measurable at 200 ps and covering 10 Giga sample per second with frequency bandwidth of 3 GHz. Antenna and waveguide in *U* band with cutoff frequency at 31.4 GHz for TE_{10} mode are employed to observe the temporal waveform of the radiation.

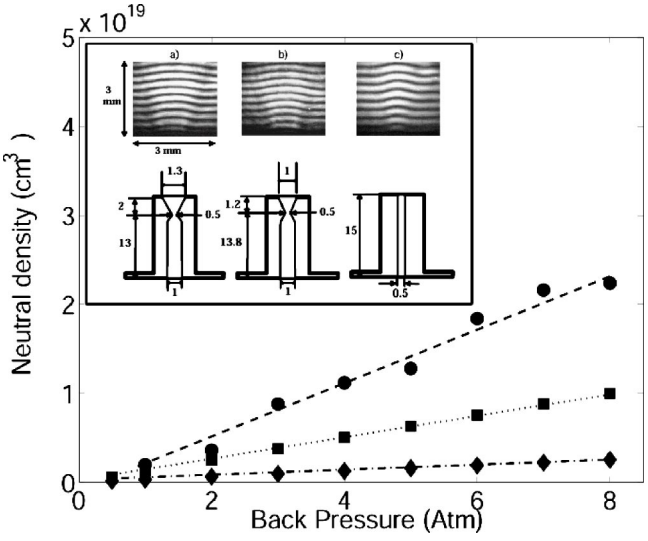

FIG. 3. Interferometer fringe shift of different nozzles are shown at the top. Diamonds on dashed dotted line, squares on dotted line, and circles on dashed line are the neutral gas density magnitudes at different back pressures of nozzles (a), (b), and (c) correspondingly.

III. INTERFEROMETER

The Mach-Zehnder interferometer is employed to detect fringe shifts due to the neutral gas density of the gas-jet flow. A He-Ne laser beam working at 632 nm is expanded and collimated to 5-mm-diameter beam which propagates in the interferometer, passed by the tip of the gas-jet nozzle. The beam splitters and mirrors of the interferometer have a surface quality of $\lambda/4$. Outside the vacuum chamber an $f/10$ spherical lens images the gas-jet through the Nd filter onto a linear charge coupled device detector. The spatial resolution is limited by the pixel size of about 15 μm. Gas jet characteristics are explained in the last chapter. The back pressure of the gas reservoir is measured by a gas pressure gauge in the range of 0.5–8 atm. In order to study the effect of nozzles on different gas density configurations, different kinds of brass nozzles in shape and size are machined. First two are supersonic nozzles at 0.5 mm throat diameter and divergence angle of 12°. For bigger one the exit hole diameter is 1.3 mm (a) and for smaller one it is 1 mm (b). Third one is a simple cylindrical nozzle at 0.5 mm throat diameter (c).

Typical patterns of the fringe shifts are shown at the top of Fig. 3. They are measured in radians and since the geometry of the nozzle and the medium can be assumed to be cylindrically symmetric, the cylindrical Abel inversion transformation is employed in order to obtain the local density in the gas flow. After the Abel inversion transformation in cylindrical coordinates, the axial data can be changed to radials. Neutral nitrogen gas density of three nozzles with different back pressures are shown in Fig. 3. Neutral gas density of nozzle (a) is from 1.5×10^{17} cm^{-3} to 2.5×10^{18} cm^{-3} at the center of the flow, and about 0.5 mm upper than the nozzle exit. For nozzle (b) this magnitude changes from 6.5×10^{17} cm^{-3} to 1×10^{19} cm^{-3} and for nozzle (c) it is from 2×10^{18} cm^{-3} to 2.15×10^{19} cm^{-3} both at the same point. In this range of the back pressure of the supplied gas, the gas density is a linear function of the back pressure. According to laser intensity of about 10^{17} W/cm^2, gas is expected to be fully ionized and we can calculate the plasma density from neutral gas density.

The sharpest boundary between the gas flow and vacuum has been found for the case of nozzle (a) at about 0.5 mm from the nozzle tip. In this case, neutral gas density is approximately flat in the radius of about 0.4 mm and falls down to zero within 0.1 mm. We cannot generate the ideally sharp boundary due to the quick expansion of the gas flow, which occurs at the nozzle exit. Indeed, this effect occurs due to the very low background pressure in the vacuum chamber, so the flow is said to be ''underexpanded'' and a subsequent expansion occurs as the flow attempts to meet the necessary boundary condition imposed by the ambient chamber background pressure [17].

IV. RESULTS AND DISCUSSION

In Fig. 4 a typical radiation waveform is shown, obtained from helium plasma at $B_0=7.8$ kG, that corresponds to $\omega_c=1.4\times10^{11}$ rad/s. The observed pulse duration of the order

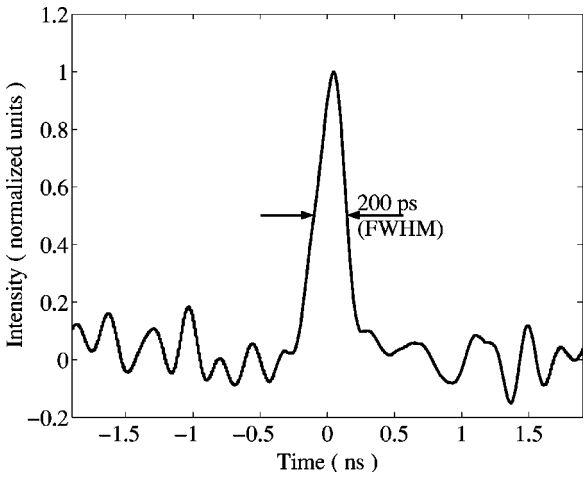

FIG. 4. Sample of the radiation pulse.

of 200 ps at FWHM is limited by the bandwidth of the receiving equipment. From nitrogen plasma, the similar result is also obtained. The lifetime of the wakes in the plasma can be estimated from $\tau_p\sim L_p/v_g$, where L_p is the plasma length of the order of Rayleigh length and v_g is the group velocity of the wakes in the plasma. In this experiment with laser spot size of 20 μm, L_p is estimated to be about 1.55 mm. The electron density is about 10^{17} cm^{-3} correspondingly $\omega_p\simeq1.8\times10^{13}$ rad/s, so τ_p should be about 80 ns theoretically. But experimental results show that wakefield disappears faster than the calculated lifetime. In a similar experiment, the calculated lifetime for wakes is about 5.4 ns while the lifetime of the plasma waves, measured by Thomson scattering, is about 300 ps [18]. The reason could be explained by taking into account the gas ionization effect. In the case of performed plasma, whose volume is larger than the laser pulse perturbation volume, when a corona electron moves away from its first position, a positive charge is created. This induces a restoring electrostatic force that is proportional to the electron displacement and produces a harmonic oscillator system at the plasma frequency. On the other hand, in the tunnel ionization produced plasma, when the corona electron leaves the plasma, the number of positive charges is fixed by the laser pulse radius and Rayleigh length. Laser pulse energy is more nonuniform in this volume and electrons feel more nonuniform force. This could induce a lower restoring electrostatic force and larger number of electrons which do not come back in phase with plasma waves and destroy the oscillation faster than the expected time. Similar to this effect for the radial component of plasma wakefield also has been observed [19].

The polarization of the emitted radiation is measured by rotating the receiver horn antenna around the z axis in both cases of He and N_2 plasma at different gas densities. As it is predicted by the theory, the electromagnetic component of the wakes is in the x direction perpendicular to the direction of the applied external dc magnetic field. Experimental data show that the radiation is also polarized in the x direction, in fairly good agreement with expectation.

The spatial distribution of the radiation is measured by changing the position of the horn antenna in different angles,

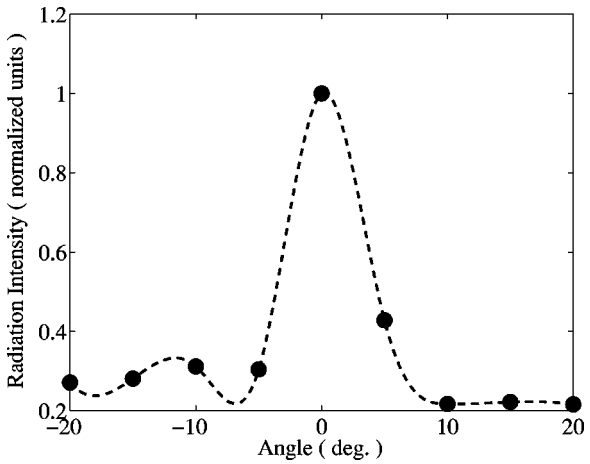

FIG. 5. Spatial distribution of the emitted radiation.

referred to the z axis in the y-z plane. Data are shown in Fig. 5. The radiation is mainly launched within the angle $\pm 5°$ with respect to the z axis in the y-z plane, in the forward direction. Pulse becomes weaker in larger angles up to $\pm 8°$ and absolutely disappears after that. These results are confirmed by the fact that the group velocity of the magnetized wake is maximum in the forward direction.

The intensity of the radiation of both He and N_2 plasmas in different densities are shown in Fig. 6. Gas density is controlled by the back pressure to the gas-jet nozzle and density is obtained in the interferometer experiment. Data are obtained by using nozzle (a) at the external magnetic field strength of about 8 kG. The base pressure of the interaction chamber is 15 mTorr, and gas-jet open time is 250 μs and 10 Hz repetition rate. One can see that the radiation intensity decreases noticeably by increasing the gas density. Radiation from other nozzles show the similar behavior.

In Fig. 7, three samples of the radiation pulses from different nozzles are displayed for comparison purposes. The position of three radiation pulses are shifted in order to simplify their comparison. Data show the radiation from N_2 plasma at 1 atm back pressure in 15 mTorr of chamber pressure and 250-μs gas-jet valve open time and 10 Hz repetition

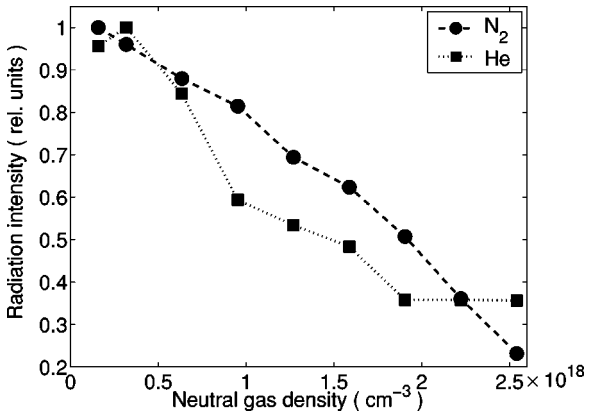

FIG. 6. Radiation intensity in relative units versus neutral gas density for both He (dotted full square line) and N_2 (dashed full circle line) plasma. The experiment is done by nozzle (a).

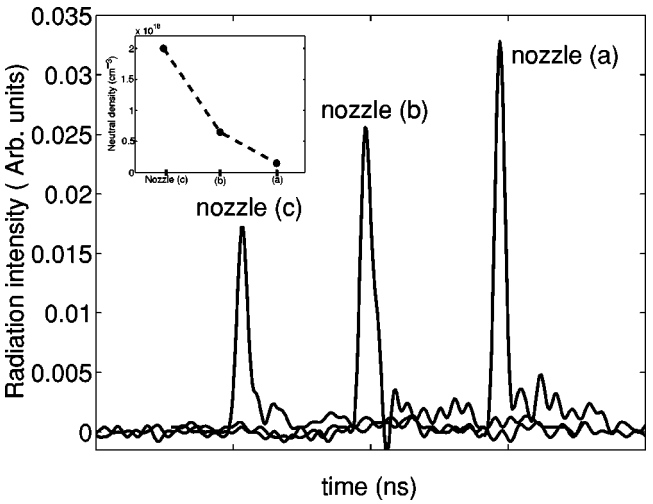

FIG. 7. Radiation intensity of three different nozzles at constant gas pressure of 15 mTorr of N_2.

rate. Here also, the lowest radiation is observed with the nozzle (c) plasma, which generates the largest density magnitude, and with decreasing the plasma density the radiation has been enhanced.

Both data in Figs. 6 and 7 verify that increasing the plasma density in this range will decrease the radiation intensity. These results can be explained from the theory clearly due to the fact that in the present experiments we deal with plasma densities greater than the laser wakefield quasiresonance. Indeed the term ''$\sin(\omega\xi_0/2)$'' in Eqs. (A7a) and (A8a) represents the quasiresonance behavior of the plasma wakefield, which confirms that increasing the plasma density from an optimum magnitude will decrease the amplitude of the plasma wakefield. Due to $\omega=\sqrt{\omega_p^2+(1-\beta^2)\omega_c^2}$ (see Appendix), when $\omega_c \ll \omega_p$ plasma wakefield frequency ω is very close to plasma frequency ω_p and the maximum wake amplitude is created when $c\tau_L=\lambda_p$, where τ_L is the laser pulse width and λ_p is the plasma wavelength. In the present experiment, the maximum of the wakefield amplitude is expected at 5 THz plasma frequency, corresponding to electron density 3.1×10^{17} cm^{-3}. Increasing the density from this optimum magnitude decreases the wakes amplitude sharply [19]. The lowest neutral densities of nozzle (a), (b), and (c) are 1.5×10^{17} cm^{-3}, 6.5×10^{17} cm^{-3}, 2×10^{18} cm^{-3}, and plasma electron densities are five times bigger for nitrogen, all of them larger than the optimum magnitudes. Decreasing the wake amplitude with increasing the density when density is larger than optimum density is in good agreement with theory of the plasma wakefield.

Relative output power of the radiation versus the external magnetic field is shown in Fig. 8. The data are obtained without changing the position of the gas-jet nozzle and the laser beam. The magnetic field is varied by changing the distance between permanent magnets pair, which are controlled from out of the vacuum chamber. The experiment is done by nozzle (a) at the constant back pressure of 1 atm, corresponds to 1.5×10^{17} cm^{-3} neutral gas density. Working gas is N_2. The circles are the average of data upon six magnitude and the error bars indicate the difference between

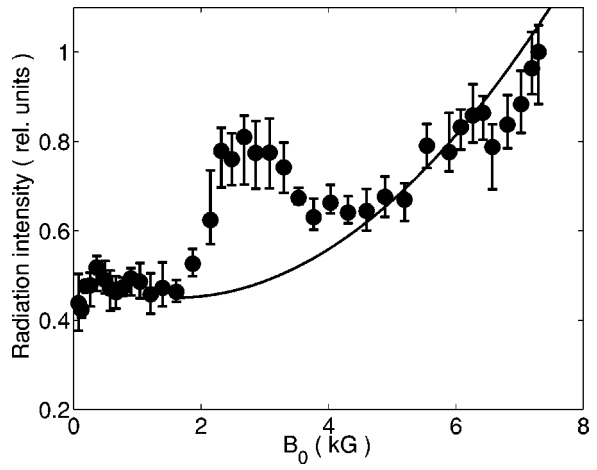

FIG. 8. Output power of the radiation as a function of the applied external dc magnetic field. Solid line indicates the theoretical value. Error bars show the difference between the maximum and minimum of the obtained experimental data.

maximum and minimum of the experimental data at each magnitude of magnetic field strength. From $B_0=0$ to 1.7 kG, although the amplitude of the signal is larger than the noise level, the radiation intensity does not change significantly with increasing the magnetic field. In this region, magnetic field is weak and unable to affect the plasma wakefield. The observed radiation in this range of B_0 might be caused by nonlinear currents [20]. Up to 7.5 kG, the output power of the radiation increases with the magnetic field strength. Solid line indicates the theoretical values. Due to Eqs. (A7a) and (A8a) the amplitude of the radiation is proportional to ω_c or B_0. So without taking the damping phenomenon into account the output power of the radiation is proportional to B_0^2. Because of the sharp boundary of the gas-jet plasma, the radiation emitted without the boundary effect, in contrast to the theory predicted by Yoshii *et al.* [13] and experimentally observed by Yugami *et al.* [14] in chamber filled gas. Due to the mentioned theory of the boundary model, the attenuation of the output power increases with B_0 faster than increasing the output power which goes as B_0^2. Up to now, the peak in radiation around $B_0=3$ kG cannot be explained.

Another effect of using the gas-jet plasma to excite the radiation is as follows. Typical radiation waveform observed by using the gas-jet flow (Fig. 4) consists of single radiation pulse of millimeter wavelength, whereas the radiation from gas-filled chamber obtained in similar experimental conditions represents a set of pulses. Number of these pulses and their relative intensities depend on experimental conditions, namely, on the gas pressure. Time-of-flight diagnostics by using a longer waveguide of about 75 cm displays the difference between two experimental approach even more clearly. In those measurements, the width of each pulse of radiation from the chamber filled gas broadens noticeably by about three times, but the pulse width of radiation from the gas-jet plasma does not change.

Broadening the pulse width of the radiation during the flight through the longer waveguide is due to different group velocities and frequencies in the pulse. Thus, the results of those measurements indicate the wide frequency range of the radiation from the gas-filled chamber, whereas radiation from the gas-jet flow is found to be quasimonochromatic. Difference can be because of the nonuniform plasma density in the case the gas-filled chamber, while the gas-jet plasma characterizes by uniform density and sharp boundary. In other words, it shows the effect of gas-jet nozzle in localizing the gas and generating the plasma with uniform density and sharp boundary.

From another point of view, by estimating the plasma length $L_p \approx 1.5$ mm and plasma lifetime less than 200 ps, we can see only that part of the wake whose group velocity in the axial direction is about 10^9 cm/s or more are taken part in the radiation, but it is well known that in order to produce wakefield with larger amplitude we need to focus the beam in a smaller spot, so the wake group velocity decreases in the axial direction and increases in the radial direction, which leads to dissipating a part of wakefield energy in the plasma.

Furthermore, in the present experiment, the maximum magnetic field applied is about 8 kG, corresponding to cyclotron frequency $\omega_c=1.4\times10^{11}$ rad/s. Therefore, the assumption of $\omega_H^2=\omega_p^2+\omega_c^2\simeq\omega_p^2$ as $\omega_c \ll \omega_p$ is quite natural and the present wakefield scheme is exactly the same situation as the $\mathbf{V}_p\times\mathbf{B}$ acceleration scheme, which was originally introduced as the plasma based high energy acceleration scheme [21–24]. In the presence of the static magnetic field, the electrostatic plasma waves travel across the magnetic field lines and accelerates the trapped electrons very efficiently by the $\mathbf{V}_p\times\mathbf{B}$ mechanisms, where $\mathbf{V}_p$ is the phase velocity of the electron plasma wave and $\mathbf{B}$ is the steady magnetic field intensity. In other words, the $\mathbf{V}_p\times\mathbf{B}$ radiation scheme is the inverse process of $\mathbf{V}_p\times\mathbf{B}$ acceleration mechanism. In this sense, the $\mathbf{V}_p\times\mathbf{B}$ radiation decreases the acceleration efficiency, but this is negligibly small compared with the acceleration efficiency, and no serious losses take place for the particle accelerators, if the trapped particles in the wave frame are small in number, i.e., the loading effect is small enough.

V. CONCLUSION

Short pulse radiation from the interaction of short intense laser pulse and magnetized gas-jet plasma is investigated as a new source of coherent radiation tunable in frequency pulse duration and intensity. Different radiation characteristics, specially dependence of the radiation intensity on plasma density have been studied. By using gas-jet flow to generate the plasma, the effect of the sharp plasma boundary on the radiation intensity is investigated. Increasing the radiation intensity with magnetic field strength confirms the uniformity of the plasma density and sharpness of the gas-jet plasma boundary.

ACKNOWLEDGMENTS

We would like to thank Professor Michael I. Bakunov with Department of Radiophysics, University of Nizhny Novgorod, Russia for his very useful discussions and Dr. Higashiguchi with Department of Electrical and Electronic

Engineering, Miyazaki University of Japan for his useful technical support. We are also grateful to Cooperative Research Center and Satellite Venture Business Laboratory (SVBL) of Utsunomiya University for providing us the laser system. One of the authors (M.S.) is grateful to SVBL for providing the financial support. A part of the work was supported by the Grant-in-Aid in Scientific Research from the Ministry of Education, Culture, Sports, Science and Technology, Japan.

APPENDIX: MAGNETIZED WAKE CALCULATIONS

It is convenient to review the theory presented originally by Yoshii *et al.* [13], modified after taking into account our experimental conditions. In contrast to the original theory, where all transversal components of the magnetized wake have been found through perturbation technique, we have developed a direct analytical procedure, which allows us to find exact expressions for all components of magnetized plasma wake. These expressions can be used for any driver velocities as well as for any ratios of ω_c/ω_p. The radiation geometry is presented in Fig. 2. Laser pulse propagates in the z direction and external dc magnetic field is applied in the y direction. This field is uniform in space and constant in time. Maxwell's equations for plane waves in one dimension for the present geometry have the form, in the first-order relationship,

$$-\frac{\partial E_x}{\partial z}=\frac{1}{c}\frac{\partial B_y}{\partial t}, \tag{A1a}$$

$$-\frac{\partial B_y}{\partial z}=\frac{1}{c}\frac{\partial E_x}{\partial t}-\frac{4\pi}{c}eNV_x, \tag{A1b}$$

$$\frac{1}{c}\frac{\partial E_z}{\partial t}-\frac{4\pi}{c}eNV_z=0. \tag{A1c}$$

Then, first-order velocities V_x and V_z are the components of electron velocity satisfying the equation of motion:

$$m\frac{\partial V_x}{\partial t}=-eE_x+\frac{e}{c}B_0V_z, \tag{A2a}$$

$$m\frac{\partial V_z}{\partial t}=-eE_z-\frac{e}{c}B_0V_x-e\frac{\partial \phi}{\partial z}. \tag{A2b}$$

Here, B_0 is the applied external dc magnetic field magnitude and ϕ is the average ponderomotive potential defined by the laser pulse envelope. It can be assumed that the potential ϕ and therefore the fields and electrons velocity are functions of only $\xi=t-z/v_0$, where v_0 is the initial phase velocity of wakes. This implies that pump depletion and laser instabilities are neglected. In terms of new variable, applying Laplace transformation with respect to ξ, the set of Eqs. (A1) and (A2) become

$$\tilde{E}_x=\beta\tilde{B}_y, \tag{A3a}$$

$$s\tilde{B}_y=s\beta\tilde{E}_x-4\pi e\beta N\tilde{V}_x, \tag{A3b}$$

$$s\tilde{E}_z=4\pi eN\tilde{V}_z, \tag{A3c}$$

$$s\tilde{V}_x=-\frac{e}{m}\tilde{E}_x+\omega_c\tilde{V}_z, \tag{A3d}$$

$$s\tilde{V}_z=-\frac{e}{m}\tilde{E}_z-\omega_c\tilde{V}_x+\frac{e}{\beta mc}s\varphi, \tag{A3e}$$

where tilde refers to Laplace transformation of variables, s is the Laplace variable, φ is the Laplace transformation of ϕ, and $\beta=v_0/c$. Answers for set of Eq. (A3) are

$$\tilde{E}_x(s)=\beta\tilde{B}_y(s)=\frac{\beta\omega_c\omega_p^2}{cD(s)}\varphi, \tag{A4a}$$

$$\tilde{E}_z(s)=\frac{\omega_p^2\beta^2-s^2(1-\beta^2)}{s\omega_c\beta^2}\tilde{E}_x(s), \tag{A4b}$$

where as usual ω_p and ω_c are the plasma frequency and electron cyclotron frequency, respectively. $D(s)=[\epsilon\beta^2\omega_p^2-(1-\beta^2)(s^2+\omega_p^2+\omega_c^2)]$, in which $\epsilon=1+\omega_p^2/s^2$. The inverse Laplace transformation of the above equations gives the components of the excited magnetized wakes behind the laser pulse. They are described by the residue of Eq. (A4a) at the pole where $D(s)=0$. The dispersion equation $D(i\omega)=0$ defines the frequency ω of the wake field. The amplitude of the field B_y is given at the pole $s=i\omega$ and takes the following form:

$$B_y=\frac{i\omega^3\omega_c\omega_p^2}{2c[\omega_p^4\beta^2+(1-\beta^2)\omega^4]}\varphi(i\omega). \tag{A5}$$

For laser pulse of duration τ, electric field E_L and frequency ω_L, ponderomotive potential has the form $\phi=eE_L^2/4m\omega_L^2$. Transforming it to ω space, for the longitudinal component of magnetized wakes, the electric field can be expressed via the relation

$$E_z=\frac{\omega_p^2\beta^2+(1-\beta^2)\omega^2}{i\omega\omega_c\beta}B_y, \tag{A6}$$

also taking into account the contribution of another pole at $s=-i\omega$, the final relation for magnetized wakes transverse and longitudinal components can be obtained as

$$E_x=\frac{eE_L^2}{2mc\omega_L^2}\frac{\beta\omega^2\omega_c\omega_p^2}{\omega_p^4\beta^2+(1-\beta^2)\omega^4}\sin\frac{\omega\xi_0}{2}\sin\left(\omega\xi-\frac{\omega\xi_0}{2}\right), \tag{A7a}$$

$$E_z=-\frac{eE_L^2}{2m\omega_L^2v_0}\frac{\omega\omega_p^2[\omega_p^2\beta^2+(1-\beta^2)\omega^2]}{\omega_p^4\beta^2+(1-\beta^2)\omega^4}\times\sin\frac{\omega\xi_0}{2}\cos\left(\omega\xi-\frac{\omega\xi_0}{2}\right), \tag{A7b}$$

in which $\xi_0=\tau_L-z/v_0$. τ_L is the laser pulse time. These equations can be used for any radiation driver, i.e., electron bunch or laser pulse with different velocities.

When $\omega_p \gg \omega_c$ is assumed, following the present experimental conditions, one obtains $\omega=\sqrt{\omega_p^2+(1-\beta^2)\omega_c^2}$ for the radiation frequency and Eqs. (A7a) and (A7b) are converted to

$$E_x=\frac{eE_L^2}{2mc\omega_L^2}\frac{\beta\omega_c[\omega_p^2+(1-\beta^2)\omega_c^2]}{\omega_p^2+2(1-\beta^2)^2\omega_c^2}\sin\frac{\omega\xi_0}{2}\sin\left(\omega\xi-\frac{\omega\xi_0}{2}\right), \tag{A8a}$$

$$E_z=-\frac{eE_L^2}{2m\omega_L^2 v_0}\frac{\omega_p[1+(1-\beta^2)(3/2-\beta^2)\omega_c^2/\omega_p^2]}{\omega_p^2+2(1-\beta^2)^2\omega_c^2}\times\sin\frac{\omega\xi_0}{2}\cos\left(\omega\xi-\frac{\omega\xi_0}{2}\right). \tag{A8b}$$

In this case, $\omega_H \simeq \omega_p$ and the dispersion relation reduces to $c^2k^2/\omega^2 \simeq 1-\omega_p^2/\omega^2$ and the ratio of em component of the field to es component is

$$\left|\frac{E_x}{E_z}\right|=\beta^2\left[1-(1-\beta^2)^2\frac{\omega_c^2}{\omega_p^2}\right]\frac{\omega_c}{\omega_p}. \tag{A9}$$

[1] I.Y. Dodin and N.J. Fisch, Phys. Rev. Lett. **88**, 165001 (2002).
[2] H. Lin, L.M. Chen, and J.C. Kieffer, Phys. Rev. E **65**, 036414 (2002).
[3] P. Ji, Phys. Rev. E **64**, 036501 (2001).
[4] O.F. Hagena and W. Obert, J. Chem. Phys. **56**, 1793 (1972).
[5] A. Modena, Z. Najmudin, A.E. Dangor, C.E. Clyton, and K.A. Marsh, Nature (London) **337**, 606 (1995).
[6] C.A. Coverdale, C.B. Darrow, C.D. Decker, W.B. Mori, K.C. Teng, K.A. Marsh, C.E. Clyton, and C. Joshi, Phys. Rev. Lett. **74**, 4659 (1995).
[7] S.D. Baton, F. Amiranoff, V. Malka, A. Modena, M. Salvati, C. Coulaud, C. Rousseaux, N. Renard, P. Mounaix, and C. Stenz, Phys. Rev. E **57**, 4895 (1998).
[8] J. Denavit and D.W. Phillion, Phys. Plasmas **1**, 1971 (1994).
[9] H. Fiedorowics, A. Bartnik, Z. Patron, and P. Parys, Appl. Phys. Lett. **62**, 2778 (1994).
[10] E. Fill, S. Borgstrom, J. Larson, T. Starczewski, and C.G. Svanberg, Phys. Rev. E **51**, 6016 (1995).
[11] Y.M. Li and R. Fedosejevs, Meas. Sci. Technol. **5**, 1197 (1994).
[12] V. Malka, C. Couland, J.P. Geindre, V. Lopez, Z. Najmudin, D. Neely, and F. Amiranoff, Rev. Sci. Instrum. **71**, 2329 (2000).
[13] J. Yoshii, C.H. Lai, T. Katsouleas, C. Joshi, and W.B. Mori, Phys. Rev. Lett. **79**, 4194 (1997).
[14] N. Yugami, T. Higashiguchi, H. Gao, S. Sakaii, K. Takahashi, H. Ito, Y. Nishida, and T. Katsouleas, Phys. Rev. Lett. **89**, 065003 (2002).
[15] F. Chen, *Introduction to Plasma Physics and Controlled Fusion* (Plenum, New York, 1984).
[16] P. Muggli, J. Yoshii, T. Katsouleas, C.E. Clyton, and C. Joshi, Proceedings of the 1999 Particle Accelerator Conference, New York, edited by A. Luccio and W. Mackay (IEEE, New York, 1999), Vol. 1, p. 3654.
[17] D.C. Wilcox, *Basic Fluid Mechanics*, 2nd ed. (DCW Industries Inc., California, 2000).
[18] P. Muggli *et al.*, in *Proceedings of the 29th IEEE International Conference on Plasma Science, Banff, Alberta, Canada, May 2002* (IEEE, 2002), poster 6P08, p. 297.
[19] J.R. Marques, F. Dorchies, F. Amiranoff, P. Audebert, J.C. Gauthier, and J.P. Geindre, Phys. Plasmas **5**, 1162 (1998).
[20] H. Hamster, A. Sullivan, S. Gordon, W. White, and R.W. Falcon, Phys. Rev. Lett. **71**, 2725 (1993).
[21] Y. Nishida, M. Yoshizumi, and R. Sugihara, Phys. Lett. **105B**, 300 (1984).
[22] Y. Nishida, M. Yoshizumi, and R. Sugihara, Phys. Fluids **28**, 1574 (1985).
[23] Y. Nishida and T. Shinozaki, Phys. Rev. Lett. **65**, 2386 (1990).
[24] T. Katsouleas and J.M. Dawson, Phys. Rev. Lett. **51**, 392 (1983).